

14 **Abstract**

15 Drumlins are subglacial bedforms streamlined in the direction of ice flow. Common in
16 deglaciated landscapes, they have been widely studied providing rich information on their
17 internal geology, size, shape, and spacing. In contrast with bedform investigations elsewhere
18 in geomorphology (aeolian and fluvial dunes and ripples for example) most drumlin studies
19 derive observations from relict, and thus static features. This has made it difficult to gain
20 information and insights about their evolution over time, which likely hampers our
21 understanding of the process(es) of drumlin formation. Here we take a morphological
22 approach, studying drumlin size and spacing metrics. Unlike previous studies which have
23 focussed on databases derived from entire ice sheet beds, we adopt a space-for-time
24 substitution approach using individual drumlin flow-sets distributed in space as proxies for
25 different development times/periods. Framed and assisted by insights from aeolian and fluvial
26 geomorphology, we use our metric data to explore possible scenarios of drumlin growth,
27 evolution and interaction. We study the metrics of the size and spacing of 36,222 drumlins,
28 distributed amongst 71 flow-sets, left behind by the former British-Irish Ice Sheet, and ask
29 whether behaviour common to other bedform phenomena can be derived through statistical
30 analysis. Through characterising and analysing the shape of the probability distribution
31 functions of size and spacing metrics for each flow-set we argue that drumlins grow, and
32 potentially migrate, as they evolve leading to pattern coarsening. Furthermore, our findings
33 add support to the notion that no upper limit to drumlin size exists, and to the idea that
34 perpetual coarsening could occur if given sufficient time. We propose that the framework of
35 process and patterning commonly applied to non-glacial bedforms is potentially powerful for
36 understanding drumlin formation and for deciphering glacial landscapes.

37 **1. Introduction**

38 Natural processes often organise phenomena into regular and repetitive patterns (e.g.
39 Ball, 1999). This regularity deceptively gives the impression of a simplistic formation
40 process, but pattern-forming processes are often non-linear, with patterns emerging through
41 self-organisation due to complex, and sometimes stochastic, interactions between elements
42 (Pearson, 1993; Werner, 1999; Murray, 2003; Hillier et al., 2016). Aeolian, fluvial and
43 submarine bedforms are often held up as exemplars of natural patterns (Anderson, 1990;
44 Kocurek et al., 2010; Seminara, 2010), occurring as fields of morphologically similar and
45 regularly spaced features (Figures 1A, B and C).

46 Drumlins are subglacial bedforms elongated in the direction of ice flow (e.g. Clark et
47 al., 2009). The term drumlin is used to define the most common variant in a morphological
48 continuum of subglacial bedforms (Ely et al., 2016), and they are typically 250 to 1000 m
49 long, 120 to 300 m wide and 0.5 to 40 m in relief (Clark et al., 2009; Spagnolo et al., 2012).
50 The formation and development of drumlins remains an unanswered question of great
51 relevance to both geomorphology and glaciology, as the processes which occur at the ice-bed
52 interface govern the mechanics of fast ice flow (e.g. Clarke, 1987; Kyrke-Smith et al., 2015).
53 A plethora of hypotheses have been proposed to explain their initiation (e.g. Smalley and
54 Unwin, 1968; Boulton, 1987; Shaw et al., 1989; Hindmarsh, 1999). However, in this paper
55 we focus on the development of drumlins after they have initiated. Contrary to many prior
56 assertions and analyses that regarded drumlins as randomly positioned individuals or clusters,
57 they have recently been demonstrated to exhibit a regular and repetitive spatial organisation
58 that is characteristic of a patterned phenomenon (Clark et al., 2017; Figure 1D). This is
59 potentially important, because although the concept of patterning is long established in
60 geomorphology (e.g. Anderson, 1990; Werner and Hallet, 1993; Nield and Bass, 2007),
61 drumlins have mostly eluded consideration within this context. Thus, unlike their aeolian,
62 fluvial and marine counterparts, reviews of patterning processes do not generally consider

63 subglacial bedforms within the wider patterning context (e.g. Murray et al., 2014), perhaps
64 due to the immaturity of patterning as a line of enquiry within the subglacial bedform
65 literature. This is likely a consequence of their static and often time-integrated appearance on
66 palaeo-ice sheet beds (e.g. the superimposition of several ice flow patterns), and the alteration
67 of drumlinised landscapes by other geomorphological processes after their exposure, making
68 the identification of any patterning processes which occurred during their formation
69 challenging. Though the concept of subglacial bedforms forming as a field has been
70 considered before (e.g. Smalley and Unwin, 1968; Dunlop et al., 2008; Barchyn et al., 2016),
71 Clark et al. (2017) are the first to demonstrate that patterning is a ubiquitous property of
72 drumlins. Therefore, Clark et al. (2017) opens a new avenue of enquiry for glacial
73 geomorphologists to study drumlins, more akin to how fluvial, aeolian and marine bedforms
74 are considered, whilst simultaneously providing the wider geomorphological community with
75 an interesting, although challenging opportunity to study patterning processes. Here we build
76 upon the work of Clark et al. (2017) by using the size and shape metrics of drumlins formed
77 in different flow events to ask whether behaviour common for bedforms formed by non-
78 glacial geomorphic agents occurs during drumlin formation.

79 Unlike for fluvial, aeolian or marine bedforms, direct observation of subglacial
80 bedforms beneath (or emerging from) a modern ice mass is logistically challenging and
81 limited to a few examples (Smith et al., 2007; King et al., 2009; Johnson et al., 2010).
82 Furthermore, repeat imaging of active drumlin fields from which bedform formation and
83 pattern evolution could be deciphered has yet to be achieved. Although no longer evolving,
84 the exposed beds of palaeo-ice masses provide numerous examples of drumlin patterns that
85 are likely to preserve information about the processes that created them. This rationale, that
86 the arrangement of a field of bedforms contains information regarding their development, is
87 often adopted to decipher the arrangement of aeolian dunes within a pattern (e.g. Ewing et al.,

88 2006; Ewing and Kocurek, 2010). Recent work on subglacial bedforms has begun to consider
89 how pattern interactions may influence their size-frequency distributions. Hillier et al. (2013)
90 hypothesised that randomness during ice-sediment-water interaction at multiple locations
91 combined with simple rules could explain characteristics of their size-frequency distributions.
92 A statistical model of this was then developed in Fowler et al. (2013) and evaluated in
93 combinations with a variety of models in Hillier et al., (2016). Although exposed drumlin
94 fields are relict, making any identification of pattern-forming interactions challenging, the
95 premise of this paper is that, hidden in the size metrics of relict drumlins, there are
96 measurable properties that provide insight into the time-varying state and evolution of
97 drumlin patterns (Hillier et al., 2016). Here we study the size and spatial arrangement of
98 36,222 drumlins distributed across 71 different flow-sets of the last British-Irish Ice Sheet
99 (Clark et al., 2009; Hughes et al., 2010; 2014). Unlike previous studies that focussed on the
100 entire database (Clark et al., 2009; Hillier et al., 2013; Fowler et al., 2013), we group
101 drumlins by flow-set prior to analysis. The logic here being that flow-sets or fields represent
102 sets of drumlins at various, as yet unknown, stages of development. This allows us to further
103 examine whether behaviour commonly observed in other natural patterns can be invoked to
104 explain the arrangement and morphology of drumlins.

105

106 **2. Background and Rationale**

107 Patterns often evolve through interactions between their constituent elements (e.g.
108 Muthukumar et al., 1997; Wootton, 2001). The nature of these interactions leads patterns to
109 evolve in different ways and exhibit different overall behavioural states. Several types of
110 patterning behaviour have been observed in geomorphic systems (Kocurek et al., 2010;

111 Murray et al., 2014), providing a useful framework for this investigation into drumlins, which
112 we now briefly summarise.

113 If a pattern remains stable at the wavelength at which it initiates, this is known as
114 simple stabilisation (e.g. Cherlet et al., 2007; Murray et al., 2014). However, if individual
115 elements (e.g. dunes) typically migrate and/or grow laterally, this can lead to merging and/or
116 competition between adjacent elements and thereby reducing the number of elements in the
117 pattern. This is known as ‘coarsening’ and may stop when a stable wavelength is reached
118 (e.g. Werner and Kocurek, 1999; Coleman et al., 2005; Murray et al., 2014). Alternatively,
119 coarsening could continue perpetually until the pattern is composed of very few or, indeed, a
120 single element (e.g. Andreotti et al., 2009; Murray et al., 2014). For drumlins, we use a
121 quantification of their preserved dimensions and spacing (i.e. metrics) to address the
122 following four questions pertinent to their development within a pattern:

123 i) Do drumlins stabilise at an initial scale? In the scenario of simple stabilisation,
124 drumlins are seeded (or initiated) throughout the landscape and remain in their original
125 position without interactions occurring.

126 ii) Do drumlin patterns evolve through the growth of their elements (drumlins)? Phases
127 of drumlin growth might cause neighbouring drumlins to merge and become amalgamated,
128 i.e. coarsening.

129 iii) Do drumlins migrate? Migration of drumlins could lead to collisions and
130 coarsening.

131 iv) If there is evidence for (ii) and/or (iii), do drumlin patterns evolve toward a stable
132 coarsened state or do they perpetually coarsen? Growth (ii) and/or migration (iii) could lead
133 to either temporary coarsening, until a new stable state of the drumlin pattern is achieved, or

134 perpetual coarsening, whereby subglacial conditions favour the continuous evolution of the
135 drumlin pattern.

136

137 **3. Methods**

138 *3.1. Data acquisition*

139 Here we study the size and spacing metrics of relict drumlins, on the premise of Hillier
140 et al. (2016) that analysis of these measurable properties should provide insight into drumlin
141 evolution. As noted above, we are presently unable to fully observe drumlin formation and
142 evolution under ice sheets at appropriate time-scales (although see Johnson et al., 2010;
143 Benediktsson et al., 2016 for small sample sizes), and so we substitute space for time, which
144 is a widely-used concept elsewhere in geomorphology for deciphering landscape evolution
145 (e.g. Paine, 1985; Micallef et al., 2014). We assume that drumlin flow-sets (i.e. groups of
146 drumlins interpreted to have been formed during the same ice-flow phase), and the drumlins
147 contained within them, likely represent different (as yet unknown) stages of drumlin
148 formation, e.g. some are likely to have more mature forms, perhaps due to higher ice
149 velocities or a longer duration of flow, whereas others may contain drumlins that represent a
150 more immature stage of development. It is likely that other factors, such as sediment
151 rheological properties, sediment thickness and subglacial hydrological changes could also
152 influence the rate of drumlin pattern development. Indeed, numerical models of both
153 subglacial bedforms (Barchyn et al., 2016) and aeolian dunes (Eastwood et al., 2011) point to
154 sediment availability as being key to pattern development. These factors will be discussed
155 later. For now, our premise is that different flow-sets represent a diversity of drumlin pattern
156 maturity, but that many factors may influence pattern development. From this premise, we
157 build conceptual models of how patterning interactions may have influenced size and spacing

158 metrics of drumlins within discrete flow-sets, and compare these to measured size and
159 spacing frequency distributions.

160 In order to decipher how patterning occurs in drumlin fields, we study the size and
161 spacing metrics of drumlins formed beneath the former British sector of the British-Irish Ice
162 Sheet (Hughes et al., 2010). For each drumlin, the length, width and relief have been
163 measured previously (see Clark et al., 2009; Spagnolo et al., 2012). Here we calculated the
164 lateral (across-flow) and longitudinal (along-flow) spacing of each drumlin using the method
165 described in Stokes et al. (2013b). These measures are the shortest Euclidian distances
166 between the centre points of adjacent drumlins with respect to ice-flow direction, which is
167 defined as the average azimuth of the neighbouring 10 drumlins (Ely, 2015). Unlike previous
168 studies, which grouped all drumlins into a single database (e.g. Clark et al., 2009; Hillier et
169 al., 2013; Fowler et al., 2013), we retain the categorisation of drumlins into 100 flow-sets,
170 which were used to build a palaeo-glaciological reconstruction (Hughes et al., 2014). Thus,
171 flow-set numbers and locations are from Hughes et al. (2014) (see Table S1 for more
172 information). For the purposes of this study, we discard 29 flow-sets due to the low number
173 (< 30) of drumlins which they contain, or due to poor preservation (e.g. through cross cutting
174 or post-formational modification). The remaining 71 are analysed here, together containing
175 36,222 drumlins.

176

177 *3.2. Data processing*

178 In order to characterise the frequency distribution of each size and spacing metric
179 (length, width, relief, lateral and longitudinal spacing) within each flow-set, we extract
180 parameters based upon the description of our data following both gamma (ϕ , λ and λ) and
181 lognormal (ϕ and $\bar{\mu}$) distributions (Figure 2) (Hillier et al., 2016). First, using the method-of-

182 moment estimators detailed in Hillier et al. (2013), we compared our measurements to a
 183 gamma distribution using frequency histograms (Figure 2A). The modal value (ϕ) was
 184 calculated using the method-of-moments (Hillier et al., 2013):

$$185 \quad \phi = \frac{\left(\frac{\bar{x}}{s_x}\right)^2 - 1}{\left(\frac{\bar{x}}{(s_x)^2}\right)} \quad (1)$$

186 where \bar{x} is the mean of the distribution and s_x is the standard deviation of the data. The
 187 maximum likelihood estimator of gradient of the positive tail of the distribution (λ) was
 188 calculated by removing all data from the original dataset below ϕ to produce a subset dataset
 189 k_i (Appendix A of Hillier et al., 2013). λ is then:

$$190 \quad \lambda = 1 / \left(\frac{\sum_i(k_i - \phi)}{n}\right) \quad (2)$$

191

192 To characterise the shape of the distributions before the mode, we also define Λ , the
 193 slope of the distribution before the mode. This involved removing all values above ϕ from the
 194 original dataset, to produce K_i , and then applying the equation:

$$195 \quad \Lambda = 1 / \left(\frac{\sum_i(K_i - \phi)}{n}\right) \quad (3)$$

196 Therefore, Λ is a mirrored version of λ , with a statistical justification equivalent to that
 197 for λ (see Hillier et al., 2013). Thus, ϕ describes a modal value per flow-set, and the
 198 parameters Λ and λ describe the shape of the distribution of the flow-set. λ and Λ are
 199 independent of each other. However, Λ may be influenced by ϕ as we are studying scalar
 200 variables.

201 A second set of parameters based upon the log-normal distribution were derived using
 202 the method of Fowler et al. (2013). To calculate these parameters, the distributions were first

203 represented as histograms of frequency intensity (f_i), modified to approximate probability
204 density after Fowler et al. (2013):

$$205 \quad f_i = \frac{n_i}{n\Delta} \quad (4)$$

206 where n_i is the number of drumlins in each bin, Δ is the bin width and n is the total
207 number of the sample (Fowler et al., 2013). Bin width was kept the same for each histogram.
208 These frequency intensity histograms (Figure 2B) were visually compared to a normal
209 distribution curve in order to verify their log-normality. Secondly, the mean and variance, $\bar{\mu}$
210 and $\bar{\sigma}$, respectively, of each spacing and size variable per flow-set were defined by:

$$211 \quad \bar{\mu} = \frac{1}{n} \sum_i \ln x_i \quad (5)$$

$$212 \quad \bar{\sigma}^2 = \frac{1}{n-1} \sum_i (\ln x_i - \bar{\mu})^2 \quad (6)$$

213 3.3. Scenario-testing

214 Figure 3 outlines several conceptual scenarios of possible drumlin patterning
215 behaviour, halted at different stages of development in different flow-sets. Figure 3A outlines
216 our conceptual model of two different flow-sets which undergo simple stabilisation. In flow-
217 set 1, drumlins are initially formed and stabilise at a single size and distance apart. Different
218 ice-bed conditions in flow-set 2 mean that drumlins are formed and stabilise at a different
219 scale. This is illustrated in Figure 3A as a difference in spacing, but could equally be
220 manifested in drumlin size. Under this scenario, assuming conditions across a flow-set are
221 similar, the spread of the distributions (λ , A and $\bar{\sigma}$) is defined by little variability between
222 flow-sets, but average measures (ϕ and $\bar{\mu}$) may vary. In this case, the two flow-sets do not
223 represent different stages of maturity with a common evolution.

224 Figure 3B outlines a second conceptual model outlining a scenario whereby most
225 drumlins evolve through time by simply growing longer and without migrating, which may
226 lead to coarsening and collisions. At each successive stage drumlins grow longer, but remain
227 the same distance apart, eventually colliding and merging. If this is the behaviour that
228 characterises drumlin pattern evolution across all flow-sets, then different flow-sets, frozen at
229 different stages of growth, may show different levels of coarsening (Figure 3B). A similar
230 coarsening effect could also occur if drumlins grow wider, colliding/merging with lateral
231 neighbouring drumlins or if drumlins migrate at different rates, colliding with their upstream
232 neighbours.

233 Figure 3C illustrates a conceptual model of drumlins initially forming a set distance
234 apart, from which they then deviate due to migration, with each drumlin migrating at its own
235 pace. This assumes that migration can only occur parallel to ice flow. In this paper, we refer
236 to migration as being the movement of both the stoss and lee of drumlin (i.e. whole drumlin
237 movement), from growth of either side leading to a change in the location of the drumlin
238 centre. In the model, this leads to more variability in the longitudinal spacing of drumlins and
239 general coarsening. Again, in this conceptual model, different stages of this process are
240 imagined to be recorded in different flow-sets which have had different periods of time to
241 evolve to their observed state.

242 While the previous two cases are examples of pattern evolution that might lead to
243 perpetual coarsening, a further scenario of limited coarsening should also be tested. This is
244 the “significant pattern coarsening *en route* to a saturated wavelength” scenario of Murray et
245 al. (2014: p. 62), whereby interactions between elements cause the pattern to approach a
246 steady-state. Figure 3D illustrates a conceptual model of drumlins initially coarsening (as in
247 Figure 3B), but then reaching a size or spacing beyond which they can no longer grow. In this
248 conceptualisation, as more drumlins reach the size and spacing limit λ would increase, as the

249 formation of a tail in the distribution would be inhibited. Similar thresholds may also exist for
250 spacing, width and relief. This would lead to multiple ‘mature’ flow-sets at which drumlins
251 have reached a stable length (Figure 3D). Note that all four conceptual models are based upon
252 simplifications of drumlin development. It may be that more complex interactions, or none of
253 the proposed cases, occur and therefore dilute the signal of these simplistic expectations.

254

255 **4. Results**

256 In order to explore how drumlin size and spacing metrics vary between flow-sets, and
257 potentially decipher evolutionary sequences, the relationships between shape parameters for
258 drumlin length, derived following the method of Hillier et al. (2013), are plotted on Figure 4.
259 Similar relationships were found for width, relief, lateral and longitudinal spacing (Figures S1
260 to S4). All were found to be significant to $p \leq 0.05$ (f-test). The strongest relationships occur
261 between the parameters ϕ and λ (Figures 4A and S1 to S4), taking the form of negatively-
262 correlated power laws. This indicates that as the size or spacing of drumlins increases, the
263 gradient of the positive tail of the distribution decreases (Figure 4A). Similarly, ϕ and λ are
264 significantly highly-correlated through negative power-law relationships (Figure 4B).
265 Therefore, as drumlins get larger, or further apart, the gradient before the mode decreases.
266 This relationship is weaker for the width parameter (Figure S1). There are also significant
267 and strong correlations between λ and λ , this time taking the form of positive power laws
268 (e.g. Figure 4C). For each variable, λ is always greater than λ , indicating that the probability
269 distributions are always positively skewed. Therefore, the gamma-distribution metrics
270 indicate that size and spacing parameters change in a predictable manner between flow-sets.

271 To determine whether drumlin flow-sets are different from one another, which would
272 undermine the assumption that they represent different stages of drumlin evolution, we

273 performed analysis of variance (ANOVA) tests. Although inter-flow-set variation occurs,
274 these ANOVA tests show that there is no significant separation of flow-sets into different
275 groups or single entities (e.g. Figure 3A), despite the wide range of modal values for different
276 flow-sets (~220-740 m for length, ~100-350 m for width and ~4-12 m for relief). This means
277 that we find no highly-distinct flow-sets. Instead, they all show subtle variations from each
278 other. This is despite flow-sets being formed separately in time in space, and exhibiting a
279 range of different characteristics such as their total area, sedimentary substrate, or varying
280 degrees of underlying topographic influence.

281 To explore whether the log-normal distribution (commonly used to infer growth) can
282 describe the size and spacing of drumlins within flow-sets, we plot histograms of each metric
283 against log-normal distribution curves (Figure 5). Log-normal distributions have previously
284 been found for whole drumlin populations (Fowler et al., 2013), yet their applicability to the
285 metrics of individual flow-sets is unknown. Such distributions are often taken to infer that
286 stochastic phases of growth have occurred (Limpert et al., 2001; Fowler et al., 2013). Figure
287 5 shows how the frequency distributions of flow-sets are approximately log-normal for the
288 variables of length, width and relief. The shape of the distributions for these three variables
289 remains approximately log-normal, even for flow-sets which contain low numbers of
290 drumlins, despite the smaller sample size (Figure 5). However, the distributions of lateral and
291 longitudinal spacing do not fit a log-normal shape (Figure 5). Therefore, $\bar{\mu}$ and $\bar{\sigma}$ are poor
292 descriptors for the two spacing variables.

293 To ascertain how the shape of the distributions differs between flow-sets and, in turn,
294 establish whether any patterning interactions have occurred (Figure 3), Figure 6 plots $\bar{\mu}$
295 against $\bar{\sigma}$ for length, width and relief. We found significant positive correlations ($p \leq 0.05$, F-
296 test) for length and width, indicating that as drumlin length or width increases on average, the

297 spread of the distribution also increases (Figure 6A and B), although this relationship is
298 weaker for width. However, no such relationship was found for relief (Figure 6C).

299 To further visualise differences and the potential evolution in the shape of the
300 frequency distributions for each flow-set, Figure 7 overlays the frequency distributions of 5
301 flow-sets (see also Figure S5) chosen due to their large sample size and to characterise the
302 range of observed drumlin size metrics. For length and width, as the modal value increases,
303 its amplitude gets smaller and the spread increases (Figure 7). Conversely, modal relief
304 remains similar between flow-sets (Figure 7).

305

306 **5. Discussion**

307 We now return to the conceptual models and four questions posed in Section 2, and
308 discuss the extent to which scenarios described in Section 3.3 and illustrated in Figure 3 are
309 supported by our results.

310

311 *5.1. Do drumlins stabilise at an initial scale?*

312 One simple explanation for drumlin patterns might be that they stabilise at a set scale
313 and spacing, *without pattern coarsening*. Under this scenario, the varying shape of drumlin
314 size and spacing distributions between flow-sets would indicate that drumlins at different
315 locations were ‘printed’ at different scales onto the landscape. However, rather than
316 producing flow-sets with significantly different size and spacing metrics, we find no
317 separation of flow-sets into different statistical populations. Instead, the size and spacing
318 metrics of drumlins co-vary in an apparently continuous manner between flow-sets (Figures
319 4, S1 and S2). When characterised as gamma (Figure 4) or log-normal (Figure 7)

320 distributions, drumlin size distributions indicate that when the modal value increases, the
321 distribution becomes more widely spread. Such distributions could arise from varying
322 conditions at the ice-bed interface, or differences in process leading to a wider spread of the
323 drumlin size, shape and spacing within a flow-set as a result of simple stabilisation. However,
324 and although the mechanics of the following systems are different, similar variations in
325 distribution shape have been observed for stages of a time evolutionary sequence for other
326 phenomena (see Limpert et al., 2001), such as raindrop size (e.g. Srivastava, 1971), grain size
327 in volcanic rocks (Fowler and Scheu, 2016) and crystal size during crystallisation (e.g. Teran
328 et al., 2010; Ng, 2016). Furthermore, we find it unlikely that differences in the conditions at
329 the ice-bed interface and/or spatial variations in processes would lead to the smoothly co-
330 varying metrics that we observe here. Hence, we interpret our results as showing that drumlin
331 size and spacing evolves during development rather than from near-instantaneous ‘printing’
332 at a set scale, and we rule out simple stabilisation as a cause of differences in drumlin metrics
333 between flow-sets (Figure 3A). Indeed, we note that simple stabilisation is rarely the case for
334 natural patterns, which more often than not require evolution - growth, shrinking, interaction
335 - to yield a specific geometry or arrangement (see Murray et al., 2014; Clark et al., 2017 and
336 references therein), and are thus autogenic in nature (Clifford et al., 1993; Werner et al.,
337 2003; Pelletier et al., 2004), i.e., the pattern that emerges does so due to interactions from
338 elements within the pattern itself.

339

340 *5.2. Do drumlins grow and/or shrink?*

341 Drumlin metrics amalgamated from multiple flow-sets display log-normal or
342 exponential frequency distributions (Hillier et al., 2013; Fowler et al., 2013). This has been
343 used to infer that drumlins grow and/or shrink over time, through analogy with other

344 phenomena which display log-normal distributions (Limpert et al., 2001) and through
345 replicating the distributions predicted by statistical models (Hillier et al., 2016). Previous
346 analyses have based this interpretation on amalgamated samples from multiple ice-flow
347 events (Hillier et al., 2013; 2016; Fowler et al., 2013), which likely formed under a wide
348 variety of subglacial conditions. Rather than growing and/or shrinking over time, an
349 alternative explanation for the log-normal distribution of these multiple flow-set datasets is
350 that this simply reflects stochastically distributed subglacial parameters (e.g. effective
351 pressure, ice velocity, sediment thickness) across the multiple flow-sets from which the
352 metrics are extracted (Dunlop et al., 2008; Hillier et al., 2013; Fowler et al., 2013; Barchyn et
353 al., 2016). Our analysis of samples from individual flow-sets builds on the analysis of Hillier
354 et al., (2016), who studied the size metrics of a single flow-set and an amalgamated sample of
355 multiple flow-sets, and argued that the characteristics of drumlin frequency distributions
356 could be linked to subglacial parameters, if drumlin growth rate is known. Our work
357 indicates that drumlin size metrics are consistently positively skewed with near log-normal
358 distributions (Figures 5 and 7). This lends strong support to the hypothesis that drumlins
359 grow (or shrink) over time within the same flow-set, where one might suggest that similar
360 subglacial conditions have influenced drumlin development. While the positively skewed and
361 log-normal distributions demonstrate that either growth and/or shrinkage have occurred, the
362 fact that drumlin patterns are not the result of simple stabilisation, but are achieved through
363 drumlin interactions, indicates that these landforms must either grow and/or migrate.

364 If we assume that drumlins originate as small features (see Hillier et al., 2016), and
365 interpret different drumlin flow-set size and shape distributions as displaying an
366 evolutionary-sequence (e.g. Figures 3 and 7), then our data support the notion that there is a
367 general tendency for drumlins to get longer and wider as they develop (e.g. Figures 4, 6 and
368 7). This is consistent with the ‘cone-shaped scatter plot’ of drumlin length and width in Clark

369 et al., 2009 (see their Figure 10), and statistical models of drumlin formation (Fowler et al.,
370 2013; Hillier et al., 2016). The tight apex of the cone at lower values (and the lack of
371 datapoints below them) was taken as a fundamental initiation scale (100 metres) from which
372 drumlins were inferred to grow in length and width in various proportions to yield the overall
373 cone-shaped scatter. Consistent with the idea that drumlins originate as small features,
374 Dowling et al. (2016) propose that a set of small drumlins formed within a few years,
375 suggesting that drumlins initiate small and would naturally grow if given enough time (in this
376 case they formed as ice was quickly retreating from the region). Therefore, we interpret the
377 flow-sets with low modal size values as containing less mature drumlins.

378 Although the frequency distributions suggest that drumlin flow-sets which have had
379 more time to evolve contain longer, wider drumlins (e.g. Figure 7), we cannot rule out that
380 this general trajectory of drumlin growth is interspersed with phases of shrinking, i.e. erosion
381 (e.g. Smith et al., 2007; Hillier et al., 2016). Drumlin shrinking may even be an important
382 mechanism in drumlin pattern evolution, causing to the eventual eradication of some
383 drumlins within a pattern which would lead to pattern coarsening. Furthermore, purely
384 bedrock forms exist, which require an entirely erosional mechanism, but the extent to which
385 they are analogous to drumlins formed of unconsolidated sediments is less clear.

386 When drumlins are longer and wider within a flow-set, the spread of length and width
387 is also larger (Figures 4, 6 and 7). We interpret this as showing that, rather than all drumlins
388 growing uniformly in a flow-set, some drumlins grow longer and wider than others. Such
389 behaviour is replicated in statistical (e.g. Fowler et al., 2013; Hillier et al., 2016) and
390 numerical models (Barchyn et al., 2016). This could be related to either a variable sediment
391 supply controlling drumlin growth (e.g. Rattas and Piotrowski, 2003; Ó Cofaigh et al., 2013),
392 or drumlins initiating at different times during pattern development and thereby leading to a
393 mixed age population (e.g. Stokes et al., 2013b), or a combination of the two. The

394 preferential growth of some drumlins, at the expense of others, may lead to pattern
395 coarsening (see Section 5.5).

396 Drumlin spacing varies between flow-sets in a manner similar to the variable length
397 (Figures 4, S3 and S4), but the shapes of the distributions of spacing are not log-normal
398 (Figure 5). Therefore, drumlin spacing does not vary in the same manner as drumlin size
399 metrics. Perhaps the non-log-normal spacing distributions are a consequence of factors
400 independent from drumlin growth initially determining their placement. This is consistent
401 with a mix of regularly-seeded drumlins and ‘clones’ anchored to more randomly distributed
402 bedrock perturbations described by Clark (2010), which would produce non-log-normal
403 distributions. Another possibility is that drumlin spacing is altered due to post-formational
404 modification. That spacing is not uniform between flow-sets and varies at different locations
405 indicates that the scenario of drumlins growing longer without changing lateral spacing was
406 not detected (e.g. Figure 3B). This inference is based upon the assumption that simple
407 stabilisation does not account for the observed patterns in frequency distributions (see Section
408 5.1.). Instead, changes to the arrangement of drumlins may occur during pattern development,
409 with potential mechanisms for this being growth, erosion leading to the eradication of some
410 drumlins, amalgamation of one or more drumlins, and migration.

411 We envisage that drumlins (i.e. their relief) can grow in both net erosional and
412 depositional settings (see Clark, 2010; Stokes et al., 2013a). Where mobile sediment is
413 readily available, accretion in both the stoss and lee of a drumlin may occur (e.g. Dardis et
414 al., 1984; Fowler, 2009; Knight, 2016). Indeed, drumlins have often been reported to have
415 lee-side cavity infills (e.g. Dardis and McCabe, 1983; Dardis et al., 1984; Fisher and Spooner,
416 1994; Stokes et al., 2011; 2013a; Spagnolo et al., 2014b), indicating that lee-side deposition
417 would be an obvious mechanism via which drumlins could grow (Barchyn et al., 2016).
418 Where erosion co-exists with deposition, it is likely that sediment is transported to, and

419 deposited at, the lee of a drumlin, perhaps at the expense of relief and width (e.g. Stokes et
420 al., 2013a; Eyles et al., 2016).

421

422 *5.3. Do drumlins migrate?*

423 This question is difficult to solve using relict drumlins, but the earlier (Section 5.2.)
424 results on drumlin growth are helpful because these could also be partially or fully achieved
425 by drumlin migration. Our expectation of drumlin migration (that the spread of drumlin
426 along-flow/longitudinal spacing metrics would increase) in Figure 3C is supported by our
427 results (Figure 4). However, the spread in longitudinal spacing metrics could be attributed to
428 preferential growth of some drumlins and destruction of others. Although our data cannot
429 resolve whether or not drumlin patterns evolve through migration, a number of observations
430 from the literature are relevant to this issue. For example, some drumlins are known to be
431 composed of bedrock or gravel cores (Schoof, 2007; Stokes et al., 2011; Dowling et al.,
432 2015), indicating that the drumlin is ‘anchored’ on a core which is unlikely to have moved
433 during formation, though the surrounding sediment may have changed shape. However, other
434 drumlins contain sedimentary structures (e.g. large deformation structures) which suggest
435 they could have migrated (Boulton, 1987; Hart, 1997; Knight, 2016), and numerical models
436 predict that migration can occur (e.g. Chapwanya et al., 2011; Barchyn et al., 2016). If
437 migration or growth leads to collision, we would expect to find examples of relict drumlins
438 about to collide, or paused in mid-collision. Such arrangements are readily observed for
439 migratory dunes (Hersen and Douady, 2005; Kocurek et al., 2010), with numerical models of
440 bedforms suggesting that collisions are a key factor for regulating bedform size distribution
441 (Barchyn et al., 2016).

442 Figure 8 shows potential examples of drumlins possibly about to collide. Although
443 perhaps not as common in drumlin fields, similar typologies to those on Figure 8 have been
444 observed and modelled for colliding barchan dunes (e.g. Hugenholtz and Barchyn, 2012;
445 Parteli et al., 2014), and here we suggest that similar arrangements may be caused by drumlin
446 migration and collision. We further note that growth and migration may provide feasible
447 mechanisms to explain compound or fused drumlin typologies (e.g. Knight, 1997) and are
448 consistent with observations of downstream changes in drumlin density or ‘packing’ (Clark
449 and Stokes, 2001). Collisions may therefore be a mechanism by which pattern coarsening
450 occurs in drumlin fields. Further sedimentological and morphological studies are required to
451 examine if and how any such mobile drumlins interact.

452

453 *5.4. Do drumlins patterns evolve toward a stable coarsened state?*

454 If drumlin patterns evolve, a logical question is when do they stop evolving; do they
455 reach a final form or steady state? None of the frequency distributions observed here conform
456 to our expectation of stabilisation outlined in Figure 3D. Indeed, that all the distributions of
457 the size variables are approximately log-normal, and modal drumlin size changes from flow-
458 set to flow-set, suggests that size metrics continue to evolve (Figure 6). A similar result was
459 found in the statistical modelling of Hillier et al. (2016). This apparent lack of an upper limit
460 for drumlin length is consistent with the idea of a subglacial bedform continuum (Aario,
461 1987; Rose, 1987; Ely et al., 2016), whereby drumlins merge into mega-scale glacial
462 lineations (e.g. Stokes et al., 2013b; Spagnolo et al., 2014a; 2016; Barchyn et al., 2016). That
463 relief does not show the evolutionary sequence displayed by length and width, but maintains
464 a log-normal shape with a comparable mean in all flow-sets (Figure 6 and 7) is intriguing.
465 Perhaps relief is prevented from growing higher by some, yet unknown, glaciological cause,

466 leading to early stabilisation of drumlin relief. One possibility is that this limit is imposed by
467 sediment supply, and is reached when all available sediment is contained within drumlins
468 preventing further upward growth.

469

470 *5.5. Drumlin Pattern Evolution*

471 Interpretation of our analysis of drumlin pattern interactions is summarised in Figure 9.
472 We find that drumlins do not stabilise at their initial scale (Figure 9-T1). It is more likely that
473 they initiate at a length-scales of around 100 m (Clark et al., 2009) from which they then
474 evolve and coarsen (Figure 9-T2). Coarsening is achieved through a mixture of drumlins
475 growing longer (and bumping into each other) and migrating, with some drumlins growing at
476 the expense of others (Figure 9-T3). New drumlins are continually formed during the
477 formation period, if accommodation space and sediment becomes available. Growth of
478 drumlins, especially in a lengthwise direction, leads to perpetual coarsening until conditions
479 change radically (e.g. a change in basal thermal regime from warm-based to cold-based) or
480 deglaciation occurs (Figure 9-T4). This picture of an evolving ice-bed interface is consistent
481 with numerical and statistical modelling (Chapwanya et al., 2011; Fowler et al., 2013;
482 Barchyn et al., 2016; Hillier et al., 2016) and repeat geophysical imaging of cognate
483 subglacial bedforms beneath modern ice masses, which indicates changes at decadal
484 timescales (e.g. Smith et al., 2007; King et al., 2009).

485 That pattern development occurs in drumlin fields, implies that interactions between
486 drumlins is required to create the ordered landscapes and pattern characteristics observed (see
487 also Clark et al. 2017). In dunes, these bedform interactions (or ‘communications’) are
488 facilitated by interactions at the fluid, bedform and grain scale (Kocurek et al., 2010). For
489 example, flow separation in the lee of dunes can cause scouring in the stoss of upstream

490 dunes (Endo and Taniguchi, 2004). For drumlins, a lack of observations leaves the
491 mechanisms of communication unclear, but several possible candidates exist. At the fluid
492 scale, the drag induced by the sliding of ice over drumlins (see Schoof, 2002) may alter the
493 sediment entrainment rates via shear stress alteration. At the bedform scale, the development
494 of lee-side drumlin cavities (e.g. Fowler, 2009) may regulate drumlin growth and migration
495 (Barchyn et al., 2016), in turn controlling the size and spacing of resultant drumlins.
496 Sediment supply variations may also control inter-drumlin interactions and drumlin
497 positioning. At the simplest level, sediment must be available for bedforms to initially form,
498 and be either supplied to or recycled within the system for patterning interactions to occur.
499 Inter-drumlin interactions determined at the grain scale may occur due to the streaming of
500 sediment around the flanks of a drumlin, caused by the development of drumlin relief (e.g.
501 Boyce and Eyles, 1991). This may cause spatial variability in sediment availability, whereby
502 sediment deflected around upstream drumlins leads to an increased supply downstream of an
503 inter-drumlin area. The presence of a cavity would also introduce a region in the lee of a
504 drumlin where sediment supply is limited, thus inhibiting drumlin growth directly
505 downstream. Which, if any, of the above is the cause of drumlin interaction should be the
506 topic of further study.

507 That patterning interactions occur in drumlin fields also has implications for drumlin
508 formation hypotheses, of which there are many (see Clark, 2010 for a recent review). The
509 order and predictability of patterns seems at odds with polygenetic formation hypotheses of
510 subglacial bedforms, whereby differences in sediment composition are inferred to mean that a
511 large number of equifinite, processes are responsible for subglacial bedform formation (e.g.
512 Lindén et al., 2008; Sutinen et al., 2010). Möller and Dowling (2016) provide a framework
513 for understanding how sedimentological differences may arise due to a variety of processes,
514 given the morphological similarity of drumlins. Their ‘unifying polygenetic’ model suggests

515 that differences in boundary conditions (such as sediment thickness and ice velocity) are
516 regulated by a complex set of growth and shaping processes. Here we have shown that such
517 complex processes (growth, migration, collisions) are likely to occur. However, patterning
518 provides a useful framework for understanding these processes. The ubiquity of patterning in
519 drumlin fields that we and Clark et al. (2017) find, suggests that any site-specific
520 sedimentological differences that would otherwise lead to the conclusion of polygenesis,
521 should be considered within the context of the development and interaction of the drumlin
522 pattern. The erodent layer hypothesis (Eyles et al., 2016) proposes that all drumlins are
523 formed by the abrasion of a layer of subglacial sediment into the underlying substrate. This is
524 not necessarily at odds with the observations of patterning presented here; for example,
525 erosional bedforms can also migrate and grow over time (e.g. Richardson and Carling, 2005).
526 It is, however, difficult to reconcile with observations of subglacial bedforms where sediment
527 has accreted over time (e.g. Dardis and McCabe, 1983; Knight, 1997; Spagnolo et al., 2016).
528 The instability hypothesis of drumlin formation views drumlins as the consequence of the
529 coupled flow of ice, water and sediment at the ice-bed interface and allows for both accretion
530 and erosion of bedforms (e.g. Fowler and Chapwanya, 2014). This hypothesis is rooted in the
531 observation that drumlins are arranged in patterns, and is therefore easily suited to explain
532 patterning interactions. Numerical models of ribbed moraine formation demonstrate
533 migration and coarsening occurring (Chapwanya et al., 2011), but have not yet been adapted
534 to produce such interactions for drumlins. However, the instability hypothesis is yet to be
535 supported by sedimentological observations (Spagnolo et al., 2016; McCracken et al., 2016).
536 More generally, the results presented here suggest that advances in understanding drumlin
537 formation should come from numerical modelling that includes the possibility for inter-
538 drumlin interactions (e.g. Barchyn et al., 2016).

539

540 **6. Summary and Conclusions**

541 Here we study the frequency distributions of the size and shape metrics of 36,222
542 drumlins from 71 flow-sets of drumlins to seek inferences about patterning interactions.
543 Based on concepts applied to bedform patterns in other fields, we ask whether drumlins i)
544 stabilise at an initial scale; ii) grow; iii) migrate; and, through growth and or migration, iv)
545 evolve to a stable coarsened state or perpetually coarsen. Through examination of the size
546 and spacing metrics of drumlins per flow-set, and using space-for-time substitution, our
547 interpretation is that:

- 548 i) Drumlins do not exhibit simple stabilisation, i.e. they are not fixed by a
549 wavelength that is determined during their initial growth.
- 550 ii) Drumlins likely grow over time: a process which leads to pattern coarsening.
- 551 iii) There is potential for drumlins to migrate during pattern development, which
552 likely contributes to pattern coarsening.
- 553 iv) A lack of an observable upper limit on drumlin geometry (with the possible
554 exception of their relief) leaves the potential for perpetual coarsening to occur.

555 The approach of using size, shape and positioning metrics of relict drumlins to infer
556 dynamic inter-drumlin interactions as they grow is, of course, challenging. Nevertheless we
557 suggest that the patterning that exists in drumlin fields (Clark et al., 2017) arises from
558 drumlin growth and migration, leading to pattern coarsening. This has important
559 ramifications for modelling the formation of subglacial bedforms, and demonstrates that it is
560 misleading to consider drumlins as a collection of individual landforms. Rather, models
561 should ideally address their spatial interactions within a drumlin field.

562

563 **Acknowledgements**

564 JCE would like to thank Kathy and Chris Denison for supporting his PhD. This work was
565 initiated and supported by NERC grant NE/D011175/1 led by CDC. A.L.C.H acknowledges
566 BGS NERC PhD studentship (NE/S/A/2004/12102). Colm Ó Cofaigh and Andrew Sole are
567 thanked for their comments during JCEs viva, and Andrew Fowler is thanked for useful
568 discussions. John Hillier, an anonymous reviewer and the editorial team are thanked for their
569 constructive comments.

570

571 **References**

572 Aario R. 1977. Classification and terminology of morainic landforms in Finland. *Boreas*,
573 **6**(2): 87-100.

574 Anderson RS. 1990. Eolian ripples as examples of self-organization in geomorphological
575 systems. *Earth-Science Reviews*, **29**(1): 77-96.

576 Andreotti B, Fourriere A, Ould-Kaddour F, Murray, B, Claudin, P. 2009. Giant aeolian dune
577 size determined by the average depth of the atmospheric boundary layer. *Nature*,
578 **457**(7233): 1120-1123.

579 Baitis, E, Kocurek, G, Smith, V, Mohrig, D, Ewing, RC, Peyret, AP. 2014. Definition and
580 origin of the dune-field pattern at White Sands, New Mexico. *Aeolian Research*, **15**:
581 269-287.

582 Ball P. 1999. *The Self-made Tapestry: Pattern Formation in Nature*. Oxford: Oxford
583 University Press.

584 Barchyn, T.E., Dowling, T.P., Stokes, C.R., Hugenholtz, C.H. 2016. Subglacial bed form
585 morphology controlled by ice speed and sediment thickness. *Geophysical Research*
586 *Letters* **43** 2016GL069558. DOI.<https://doi.org/10.1002/2016GL069558>.

587 Benediktsson, Í.Ö., Jónsson, S.A., Schomacker, A., Johnson, M.D., Ingólfsson, Ó., Zoet, L.,
588 Iverson, N.R., Stötter, J. 2016. Progressive formation of modern drumlins at
589 Múlajökull, Iceland: stratigraphical and morphological evidence. *Boreas* **45**: 567-583

590 Boulton, G.S. 1987. A theory of drumlin formation by subglacial sediment deformation. In
591 Menzies, J. and Rose, J. (eds.) *Drumlin Symposium*, Balkema, Rotterdam; 25-80.

592 Chapwanya, M., Clark, C. D., Fowler, A. C. 2011. Numerical computations of a theoretical
593 model of ribbed moraine formation. *Earth Surface Processes and Landforms*, **36**(8):
594 1105-1112.

595 Cherlet, J., Besio, G., Blondeaux, P., Van Lancker, V., Verfaillie, E., Vittori, G. 2007.
596 Modeling sand wave characteristics on the Belgian Continental Shelf and in the Calais-
597 Dover Strait. *Journal of Geophysical Research: Oceans*, **112**(C6).

598 Clark, C. D. (2010). Emergent drumlins and their clones: from till dilatancy to flow
599 instabilities. *Journal of Glaciology*, **56**(200), 1011-1025.

600 Clark, C.D., Stokes, C.R. 2001 Extent and basal characteristics of the M'Clintock Channel
601 Ice Stream. *Quaternary International*, **86** (1), 81-101.

602 Clark, C. D., Hughes, A. L., Greenwood, S. L., Spagnolo, M., Ng, F. S. 2009. Size and shape
603 characteristics of drumlins, derived from a large sample, and associated scaling laws.
604 *Quaternary Science Reviews*, **28**(7), 677-692.

605 Clark, C.D., Ely, J.C., Spagnolo, M., Hahn, U., Hughes, A.L.C., Stokes, C.R. 2017. Spatial
606 organisation of drumlins. *Earth Surface Processes and Landforms*,
607 doi: [10.1002/esp.4192](https://doi.org/10.1002/esp.4192). [online] Available from:
608 <http://onlinelibrary.wiley.com/doi/10.1002/esp.4192/full>.

609 Clarke, G. K. 1987. Subglacial till: a physical framework for its properties and processes.
610 *Journal of Geophysical Research: Solid Earth*, 92(B9), 9023-9036.

611 Clifford, N.J., 1993. Formation of riffle—pool sequences: field evidence for an autogenetic
612 process. *Sedimentary Geology*, 85(1), pp.39-51.

613 Coleman, S. E., Zhang, M. H., Clunie, T. M. 2005. Sediment-wave development in subcritical
614 water flow. *Journal of Hydraulic Engineering*, 131(2), 106-111.

615 Dardis, G. F., McCabe, A. 1983. Fades of subglacial channel sedimentation in late-
616 Pleistocene drumlins, Northern Ireland. *Boreas*, 12(4), 263-278.

617 Dardis, G. F., McCabe, A. M. Mitchell, W. I. 1984. Characteristics and origins of lee-side
618 stratification sequences in late pleistocene drumlins, northern Ireland. *Earth Surface
619 Processes and Landforms*, 9(5), 409-424.

620 Dowling, T. P. F., Spagnolo, M. Möller, P. 2015. Morphometry and core type of streamlined
621 bedforms in southern Sweden from high resolution LiDAR. *Geomorphology*, 236, 54-
622 63.

623 Dowling, T. P. F., Möller, P. Spagnolo, M. 2016. Rapid subglacial streamlined bedform
624 formation at a calving bay margin. *Journal of Quaternary Science*, 31, 8, 879-892.

625 Dunlop, P., Clark, C. D. and Hindmarsh, R. C. (2008). Bed ribbing instability explanation:
626 testing a numerical model of ribbed moraine formation arising from coupled flow of ice

627 and subglacial sediment. *Journal of Geophysical Research: Earth Surface* (2003–
628 2012), 113(F3).

629 Ely, J.C. 2015. *Flow Signatures on the Bed and the Surface of Ice Sheets*, Unpublished PhD
630 Thesis. University of Sheffield; 300 pp. Ely, J.C., Clark, C.D., Spagnolo, M., Stokes,
631 C.R., Greenwood, S.L., Hughes, A.L., Dunlop, P. and Hess, D. (2016). Do subglacial
632 bedforms comprise a size and shape continuum? *Geomorphology*, 257, pp.108-119.

633 Endo N., Taniguchi K. 2004. Observations of the whole process of interaction between
634 barchans by fume experiments. *Geophysical Research Letters* 31: L12503.

635 Ewing, R.C., Kocurek, G. and Lake, L.W., 2006. Pattern analysis of dune- field
636 parameters. *Earth Surface Processes and Landforms*, 31(9), pp.1176-1191.

637 Ewing, R.C. and Kocurek, G.A., 2010. Aeolian dune interactions and dune- field pattern
638 formation: White Sands Dune Field, New Mexico. *Sedimentology*, 57(5), pp.1199-1219.

639 Eyles, N., Putkinen, N., Sookhan, S. and Arbelaez-Moreno, L., 2016. Erosional origin of
640 drumlins and megaridges. *Sedimentary Geology*, 338, pp.2-23.

641 Fisher, T.G. and Spooner, I., 1994. Subglacial meltwater origin and subaerial meltwater
642 modifications of drumlins near Morley, Alberta, Canada. *Sedimentary Geology*, 91(1),
643 pp.285-298.

644 Fowler, A. C. (2009). Instability modelling of drumlin formation incorporating lee-side
645 cavity growth. In *Proceedings of the Royal Society of London A: Mathematical,*
646 *Physical and Engineering Sciences*, 465, 2109, 2681-2702.

647 Fowler, A. C., Spagnolo, M., Clark, C. D., Stokes, C. R., Hughes, A. L. C., and Dunlop, P.
648 (2013). On the size and shape of drumlins. *GEM-International Journal on*
649 *Geomathematics*, 4(2), 155-165.

650 Fowler, A. C. and Chapwanya, M. (2014). An instability theory for the formation of ribbed
651 moraine, drumlins and mega-scale glacial lineations. In *Proceedings of the Royal*
652 *Society of London A: Mathematical, Physical and Engineering Sciences*, 470, No.
653 2171, 20140185.

654 Fowler, A.C. and Scheu, B. (2016). A theoretical explanation of grain size distributions in
655 explosive rock fragmentation. In *Proceedings of the Royal Society of London A:*
656 *Mathematical, Physical and Engineering Sciences*, 472, No. 2190, 20150843.

657 Hart, J. K. (1997). The relationship between drumlins and other forms of subglacial
658 glaciotectionic deformation. *Quaternary Science Reviews*, 16(1), 93-107.

659 Hersen, P. and Douady, S., 2005. Collision of barchan dunes as a mechanism of size
660 regulation. *Geophysical Research Letters*, 32(21).

661 Hillier, J. K., Smith, M. J., Clark, C. D., Stokes, C. R. and Spagnolo, M. 2013. Subglacial
662 bedforms reveal an exponential size–frequency distribution. *Geomorphology*, 190, 82-
663 91.

664 Hillier, J.K., Kougioumtzoglou, I.A., Stokes, C.R., Smith, M.J., Clark, C.D. and Spagnolo,
665 M.S., 2016. Exploring explanations of subglacial bedform sizes using statistical
666 models. *PloS one*, 11(7), p.e0159489.

667 Hindmarsh, R.C., 1999. Coupled ice–till dynamics and the seeding of drumlins and bedrock
668 forms. *Annals of Glaciology*, 28(1), pp.221-230.

669 Hugenholtz, C.H. and Barchyn, T.E., 2012. Real barchan dune collisions and
670 ejections. *Geophysical Research Letters*, 39(2).

671 Hughes, A. L., Clark, C. D. and Jordan, C. J. (2010). Subglacial bedforms of the last British
672 Ice Sheet. *Journal of Maps*, 6(1), 543-563.

673 Hughes, A. L., Clark, C. D. and Jordan, C. J. (2014). Flow-pattern evolution of the last
674 British Ice Sheet. *Quaternary Science Reviews*, 89, 148-168.

675 Johnson, M. D., Schomacker, A., Benediktsson, Í. Ö., Geiger, A. J., Ferguson, A. and
676 Ingólfsson, Ó. (2010). Active drumlin field revealed at the margin of Múlajökull,
677 Iceland: a surge-type glacier. *Geology*, 38(10), 943-946.

678 King, E. C., Hindmarsh, R. C. and Stokes, C. R. (2009). Formation of mega-scale glacial
679 lineations observed beneath a West Antarctic ice stream. *Nature Geoscience*, 2(8), 585-
680 588.

681 Knight, J., 1997. Morphological and morphometric analyses of drumlin bedforms in the
682 Omagh Basin, north central Ireland. *Geografiska Annaler: Series A, Physical*
683 *Geography*, 79(4), pp.255-266.

684 Knight, J., 2016. Subglacial processes from drumlins in Clew Bay, western Ireland. *Earth*
685 *Surface Processes and Landforms*, 41(2), pp.277-288.

686 Kocurek, G., Ewing, R. C., and Mohrig, D. (2010). How do bedform patterns arise? New
687 views on the role of bedform interactions within a set of boundary conditions. *Earth*
688 *Surface Processes and Landforms*, 35(1), 51-63.

689 Kyrke-Smith, T.M., Katz, R.F. and Fowler, A.C., 2015. Subglacial hydrology as a control on
690 emergence, scale, and spacing of ice streams. *Journal of Geophysical Research: Earth*
691 *Surface*, 120(8), pp.1501-1514.

692 Limpert, E., Stahel, W.A. and Abbt, M., 2001. Log-normal distributions across the sciences:
693 Keys and clues on the charms of statistics, and how mechanical models resembling
694 gambling machines offer a link to a handy way to characterize log-normal distributions,
695 which can provide deeper insight into variability and probability—normal or log-
696 normal: That is the question. *BioScience*, 51(5), pp.341-352.

697 Lindén, M., Möller, P. and Adrielsson, L., 2008. Ribbed moraine formed by subglacial
698 folding, thrust stacking and lee- side cavity infill. *Boreas*, 37(1), pp.102-131.

699 McCracken, R.G., Iverson, N.R., Benediktsson, Í.Ö., Schomacker, A., Zoet, L.K., Johnson,
700 M.D., Hooyer, T.S. and Ingólfsson, Ó., 2016. Origin of the active drumlin field at
701 Múlajökull, Iceland: New insights from till shear and consolidation
702 patterns. *Quaternary Science Reviews*, 148, pp.243-260.

703 Micallef, A., Ribó, M., Canals, M., Puig, P., Lastras, G. and Tubau, X., 2014. Space-for-time
704 substitution and the evolution of a submarine canyon–channel system in a passive
705 progradational margin. *Geomorphology*, 221, pp.34-50.

706 Möller, P. and Dowling, T.P., 2016. Streamlined subglacial bedforms on the Närke plain,
707 south-central Sweden—areal distribution, morphometrics, internal architecture and
708 formation. *Quaternary Science Reviews*, 146, pp.182-215.

709 Murray, A. B., Goldstein, E. B. and Coco, G. (2014). The shape of patterns to come: from
710 initial formation to long-term evolution. *Earth Surface Processes and Landforms*,
711 39(1), 62-70.

- 712 Muthukumar, M., Ober, C.K. and Thomas, E.L., 1997. Competing interactions and levels of
713 ordering in self-organizing polymeric materials. *Science*, 277(5330), pp.1225-1232.
- 714 Nield, J.M. and Baas, A.C.W. 2007. Modelling vegetated dune landscapes. *Geophysical*
715 *Research Letters*, 34, L06405.
- 716 Ng, F.S., 2016. Statistical mechanics of normal grain growth in one dimension: A partial
717 integro-differential equation model. *Acta Materialia*, 120, pp.453-462.
- 718 Ó Cofaigh, C., Stokes, C.R., Lian, O.B., Clark, C.D. and Tulaczyk, S., 2013. Formation of
719 mega-scale glacial lineations on the Dubawnt Lake Ice Stream bed: 2. Sedimentology
720 and stratigraphy. *Quaternary science reviews*, 77, pp.210-227.
- 721 Paine, A.D. (1985). 'Ergodic' reasoning in geomorphology: time for a review of the term?
722 *Progress in Physical Geography*, 9(1), pp.1-15.
- 723 Parteli, E.J., Durán, O., Bourke, M.C., Tsoar, H., Pöschel, T. and Herrmann, H., 2014.
724 Origins of barchan dune asymmetry: Insights from numerical simulations. *Aeolian*
725 *Research*, 12, pp.121-133.
- 726 Pearson, J. E. (1993). Complex patterns in a simple system. *Science*, 261(5118), 189-192.
- 727 Pelletier, J.D., 2004. Persistent drainage migration in a numerical landscape evolution
728 model. *Geophysical Research Letters*, 31(20).
- 729 Rattas, M. and Piotrowski, J. A. (2003). Influence of bedrock permeability and till grain size
730 on the formation of the Saadjärve drumlin field, Estonia, under an east-Baltic
731 Weichselian ice stream. *Boreas*, 32(1), 167-177.
- 732 Rose, J. (1987). Drumlins as part of glacier bedform continuum. In Menzies, J. and Rose, J.
733 (eds.) *Drumlin Symposium*, Balkema, Rotterdam, 103-118.

734 Schoof, C., 2002. Basal perturbations under ice streams: form drag and surface
735 expression. *Journal of Glaciology*, 48(162), pp.407-416.

736 Schoof, C. (2007). Pressure-dependent viscosity and interfacial instability in coupled ice–
737 sediment flow. *Journal of Fluid Mechanics*, 570, 227-252.

738 Seminara, G., 2010. Fluvial sedimentary patterns. *Annual Review of Fluid Mechanics*, 42,
739 pp.43-66.

740 Shaw, J., Kvill, D. and Rains, B., 1989. Drumlins and catastrophic subglacial
741 floods. *Sedimentary Geology*, 62(2-4), pp.177-202.

742 Smalley, I.J. and Unwin, D.J., 1968. The formation and shape of drumlins and their
743 distribution and orientation in drumlin fields. *Journal of Glaciology*, 7(51), pp.377-390.

744 Smith, A. M., Murray, T., Nicholls, K. W., Makinson, K., Aðalgeirsdóttir, G., Behar, A. E.
745 and Vaughan, D. G. (2007). Rapid erosion, drumlin formation, and changing hydrology
746 beneath an Antarctic ice stream. *Geology*, 35(2), 127-130.

747 Spagnolo, M., Clark, C. D. and Hughes, A. L. (2012). Drumlin relief. *Geomorphology*, 153,
748 179-191.

749 Spagnolo, M., Clark, C. D., Ely, J. C., Stokes, C. R., Anderson, J. B., Andreassen, K.,
750 Graham, A. G. C. and King, E. C. (2014a). Size, shape and spatial arrangement of
751 mega-scale glacial lineations from a large and diverse dataset. *Earth Surface Processes
752 and Landforms*, 39(11), 1432-1448.

753 Spagnolo, M., King, E.C., Ashmore, D.W., Rea, B.R., Ely, J.C. and Clark, C.D., (2014b).
754 Looking through drumlins: testing the application of ground-penetrating radar. *Journal
755 of Glaciology*, 60(224), pp.1126-1134.

756 Spagnolo, M., Phillips, E., Piotrowski, J.A., Rea, B.R., Clark, C.D., Stokes, C.R., Carr, S.J.,
757 Ely, J.C., Ribolini, A., Wysota, W. and Szuman, I. (2016). Ice stream motion facilitated
758 by a shallow-deforming and accreting bed. *Nature Communications*, 7.

759 Srivastava, R.C., 1971. Size distribution of raindrops generated by their breakup and
760 coalescence. *Journal of the Atmospheric Sciences*, 28(3), pp.410-415.

761 Stokes, C.R., Spagnolo, M. and Clark, C.D. (2011) The composition and internal structure of
762 drumlins: complexity, commonality, and implications for a unifying theory of their
763 formation. *Earth-Science Reviews*, 107 (3), 398-422

764 Stokes, C. R., Fowler, A. C., Clark, C. D., Hindmarsh, R. C. and Spagnolo, M. (2013a). The
765 instability theory of drumlin formation and its explanation of their varied composition
766 and internal structure. *Quaternary Science Reviews*, 62, 77-96.

767 Stokes, C. R., Spagnolo, M., Clark, C. D., Cofaigh, C. Ó., Lian, O. B. and Dunstone, R. B.
768 (2013b). Formation of mega-scale glacial lineations on the Dubawnt Lake Ice Stream
769 bed: 1. size, shape and spacing from a large remote sensing dataset. *Quaternary Science*
770 *Reviews*, 77, 190-209.

771 Sutinen, R., Jakonen, M., Piekkari, M., Haavikko, P., Närhi, P. and Middleton, M., 2010.
772 Electrical-sedimentary anisotropy of Rogen moraine, Lake Rogen area,
773 Sweden. *Sedimentary Geology*, 232(3), pp.181-189.

774 Teran, A.V., Bill, A. and Bergmann, R.B., 2010. Time-evolution of grain size distributions in
775 random nucleation and growth crystallization processes. *Physical Review B*, 81(7),
776 p.075319.

777 Werner, B. T. (1999). Complexity in natural landform patterns. *Science*, 284(5411), 102-104.

778 Werner, B.T., 2003. Modeling landforms as self- organized, hierarchical dynamical
779 systems. *Prediction in geomorphology*, pp.133-150.

780 Werner, B.T. and Hallet, B. (1993). Numerical simulation of self-organized stone stripes.
781 *Nature 361*, 142-145.

782 Werner, B. T. and Kocurek, G. (1999). Bedform spacing from defect dynamics. *Geology*,
783 *27*(8), 727-730.

784 Wootton, J.T., 2001. Local interactions predict large-scale pattern in empirically derived
785 cellular automata. *Nature*, *413*(6858), pp.841-844.

786

787 **Figure Captions**

788 Figure 1. Examples of landscapes containing bedforms. In each example, note the regular and
789 repetitive placement of individual bedforms across the landscape. (A) Sand dunes located
790 within the White Sands Dune Field, USA; Lidar data, hill-shaded from the north-east (Baitis
791 et al., 2014; downloaded from opentopo.sdsc.edu). (B) Submarine dunes on the Irish Sea
792 floor; bathymetric elevation data, hill-shaded from the north-east (data from
793 <https://jetstream.gsi.ie/iwdds/map.jsp>). (C) Fluvial dunes on the Mississippi river bed, New
794 Orleans; bathymetry elevation data, hill-shaded from the north-west (downloaded from
795 [http://www.mvn.usace.army.mil/Missions/Engineering/ChannelImprovementandStabilization](http://www.mvn.usace.army.mil/Missions/Engineering/ChannelImprovementandStabilizationProgram/2013MBMR.aspx)
796 [Program/2013MBMR.aspx](http://www.mvn.usace.army.mil/Missions/Engineering/ChannelImprovementandStabilizationProgram/2013MBMR.aspx)). (D) Drumlins located North of Barnoldswick, England;
797 Nextmap digital elevation model (DEM) hill-shaded from the north-west.

798

799 Figure 2. Example frequency plots of drumlin lengths for flow-set 9 showing: A) the
800 definition of gamma-based parameters ϕ , λ and A ; and B), the definition of log-normal based
801 parameters $\bar{\mu}$ and $\bar{\sigma}$. Both were derived to summarise the probability distribution functions of
802 size and spacing metrics (length, width, relief, lateral and longitudinal spacing) per flow-set.

803

804 Figure 3. Expected influence on drumlin size and spacing metrics for different patterning
805 behaviours; notably the position of the mode and the spread and skew of the distributions. A)
806 Simple stabilisation at different scales leads to differences in spacing metrics between two
807 different flow-sets. B) Lengthwise growth leads to coarsening. Different stages of this
808 process should be recorded at different flow-sets. C) Migration would lead to an increased
809 spread of along-flow spacing metrics. D) Stabilisation of drumlin length. If drumlins reach a

810 length beyond which they cannot grow, once a threshold is reached, the histogram's positive
811 tail will steepen. Eventually all drumlins reach the growth-limit and stop growing. (SLR =
812 stable length reached).

813

814 Figure 4. The best-fit power-law relationships between gamma-based shape parameters (ϕ =
815 mode, λ = post-modal slope, λ = pre-modal slope) for length across different drumlin flow-
816 sets. Similar relationships were found for all other variables (Figures S1 to S4).

817

818 Figure 5. Examples of frequency histograms for derived variables compared to a log-normal
819 distribution (black line) for 3 different-sized flow-sets. A) Flow-set 15, n = 471, in blue; B)
820 Flow-set 45, n = 1407, in orange; C) Flow-set 65, n = 152, in green. The three examples were
821 chosen because of their different sample sizes.

822

823 Figure 6. Scatter plots between $\bar{\mu}$ and $\bar{\sigma}$ for (A) length, (B) width, (C) relief.

824

825 Figure 7. Distributions of length, width and relief variables for 5 flow-sets. See Hughes et al.
826 (2014) for numbering and location and Figure S5 for individual histograms.

827

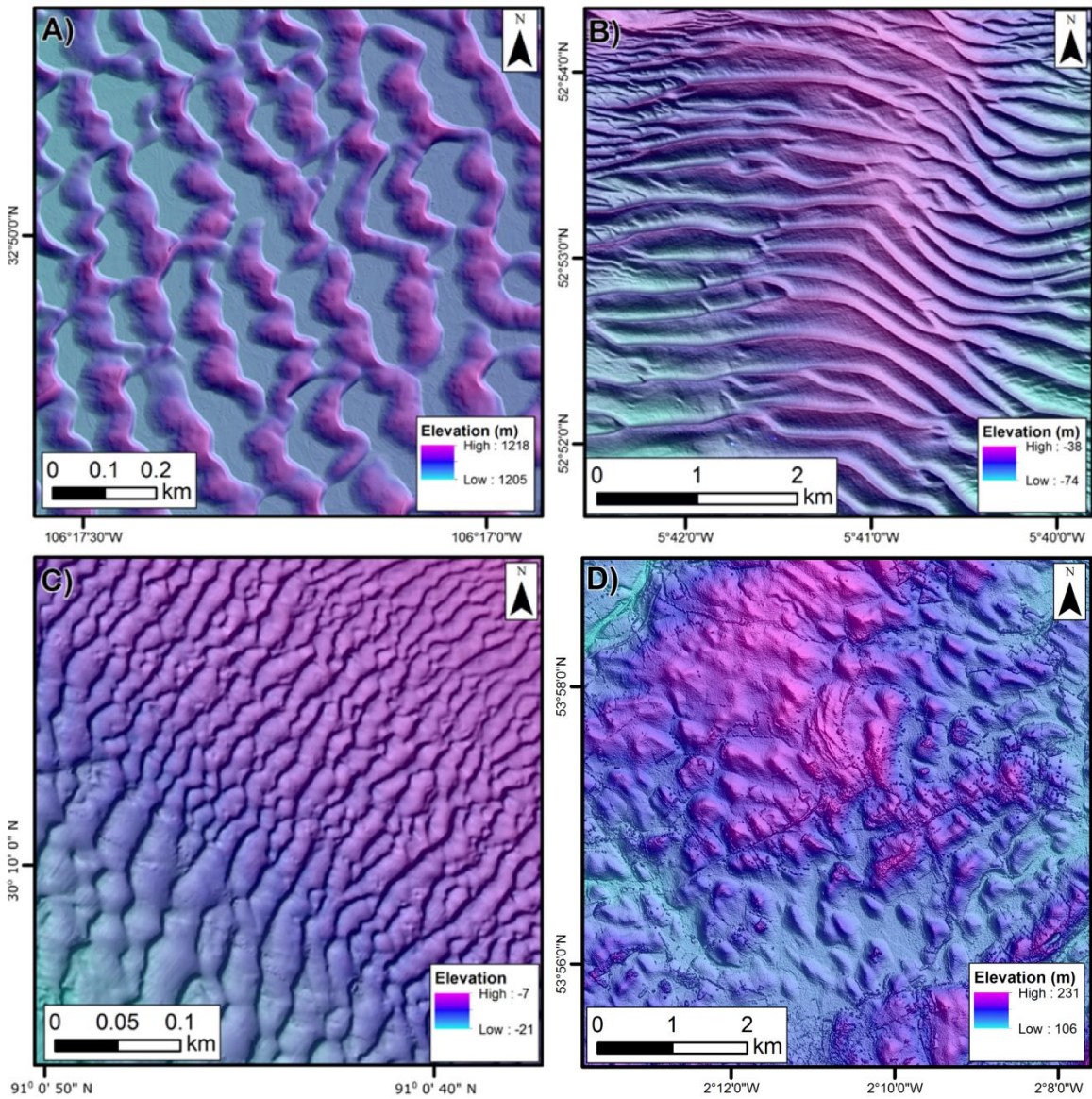
828 Figure 8. Examples of drumlins which may be mid-collision due to either growth or
829 migration. Potential collisions are labelled C. Approximate palaeo-ice flow direction denoted
830 by white arrow. Data from Nextmap DEM. (A) Instances of touching drumlins within a flow-
831 set; about to coalesce? (B) Elongate drumlins which sometimes appear to touch drumlins

832 further downstream; wholesale migration to a collision or just downstream growth? (C) Small
833 drumlins appearing to collide into the stoss side of a larger (slower moving?) drumlin. Note
834 the patch of drumlins encircled in a dashed line which may have evolved to a similar
835 arrangement if they had had longer to migrate. (D) Small drumlins which appear to have
836 collided into the stoss side of much larger drumlins.

837

838 Figure 9. Summary of potential drumlin patterning behaviour. Each box represents a different
839 stage in the evolution of the same pattern and dashed lines represent intermediate stages. At
840 T1, drumlins begin to evolve immediately, without any simple stabilisation. At T2
841 preferential growth of one drumlin leads to the amalgamation of a drumlin in its lee, whilst
842 other drumlins grow and migrate. These processes continue in T3, and new drumlins are
843 formed in the space provided by erosion of other drumlins. These processes continue until the
844 bedforms are frozen in position by deglaciation (T4), which could occur at any intermediate
845 stage.

846

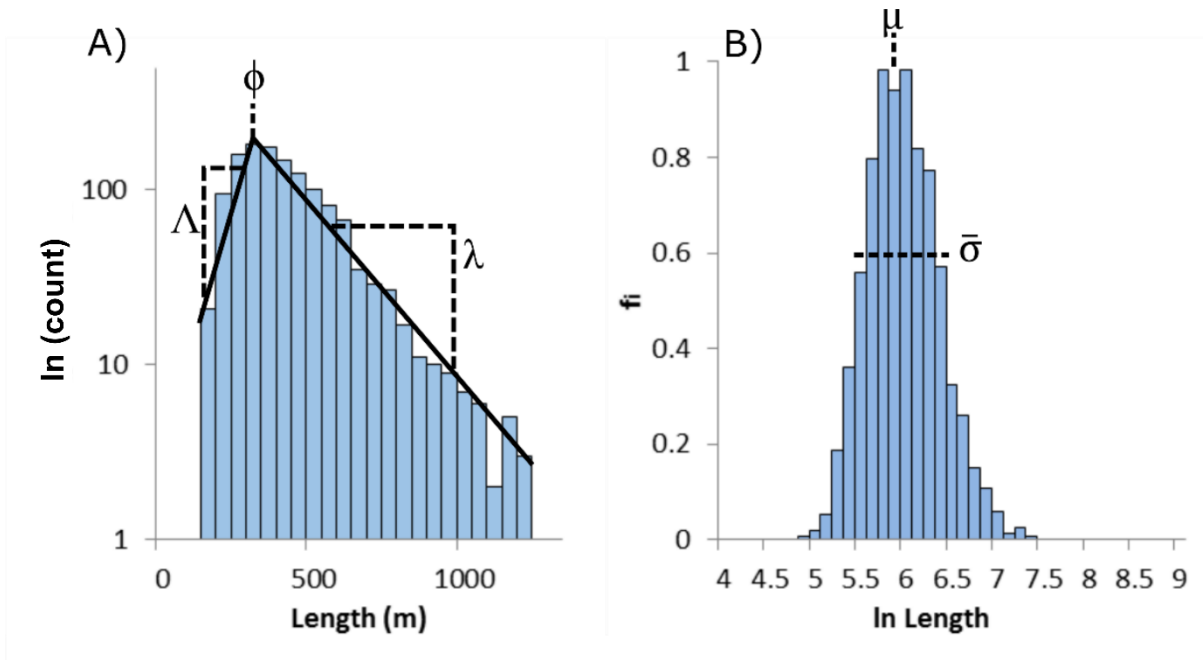


847

848

849

Figure 1

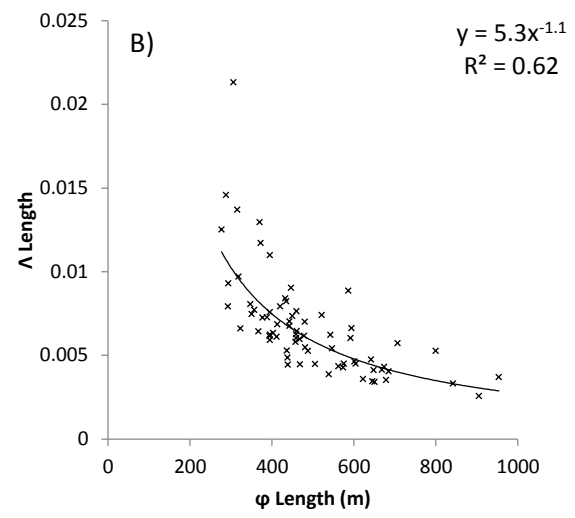
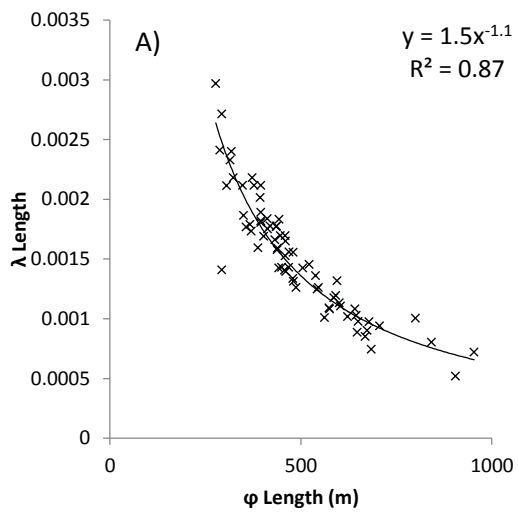


850

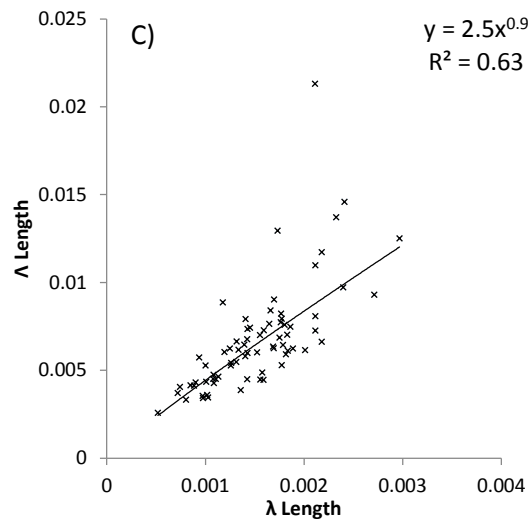
851

852

Figure 2



856

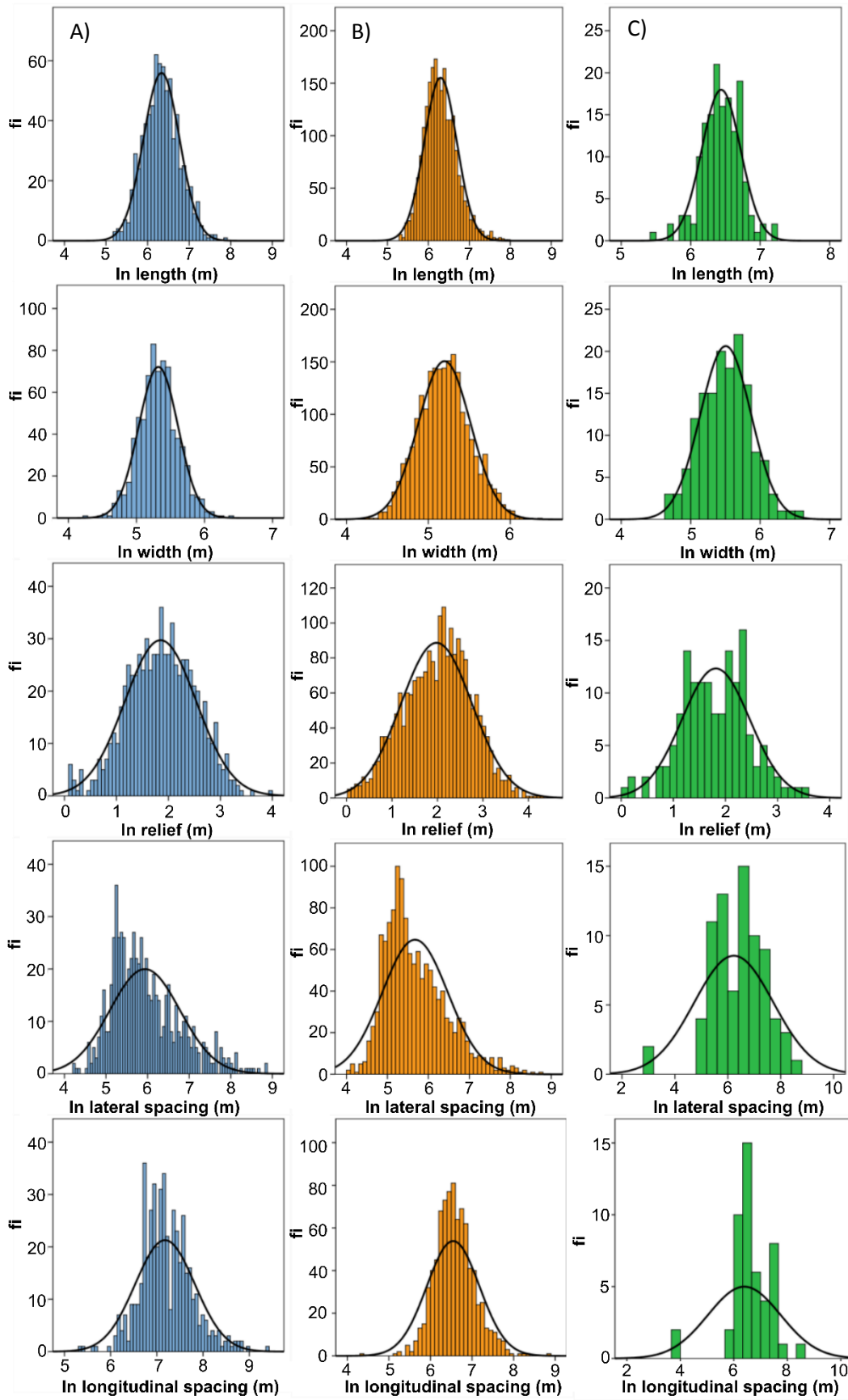


857

858

Figure 4

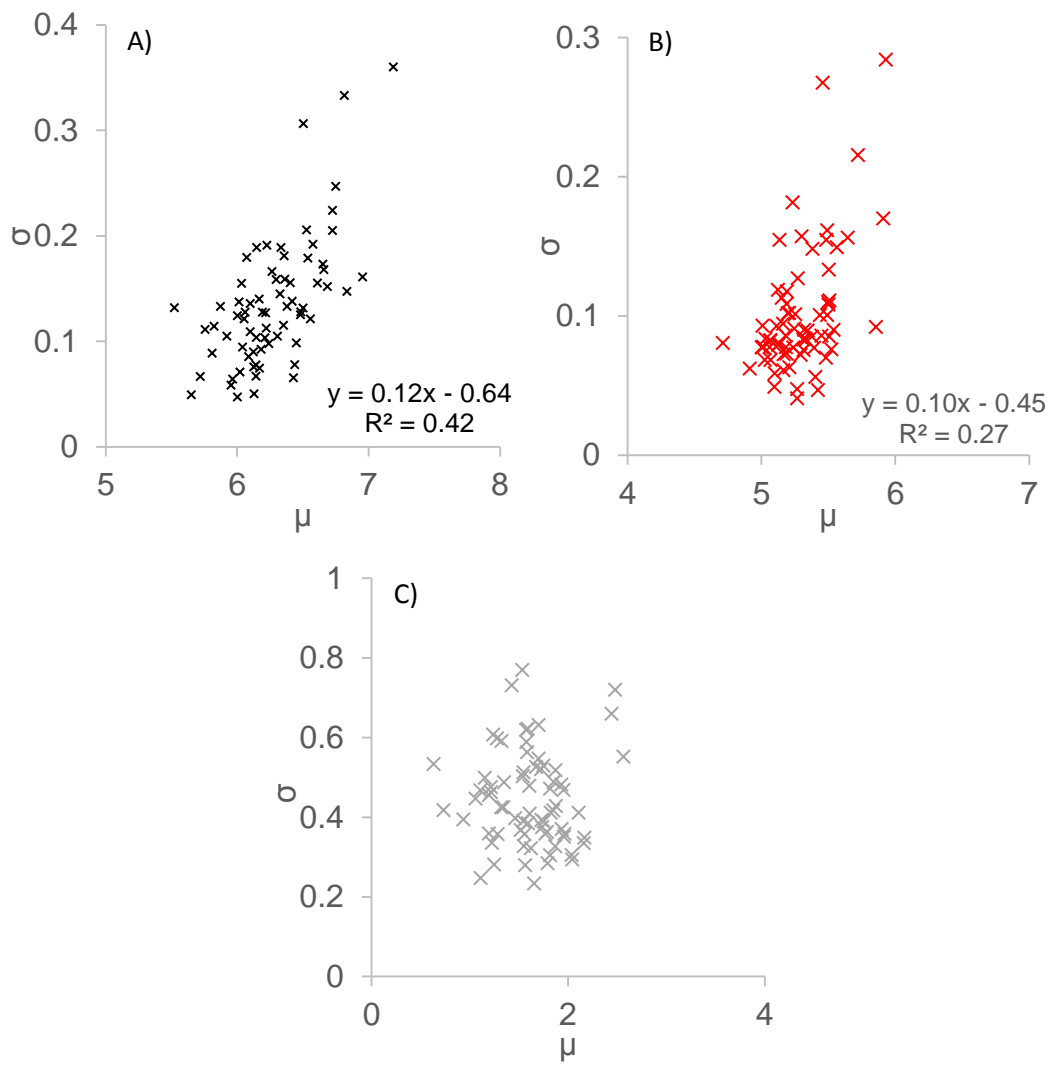
859



860

861

Figure 5



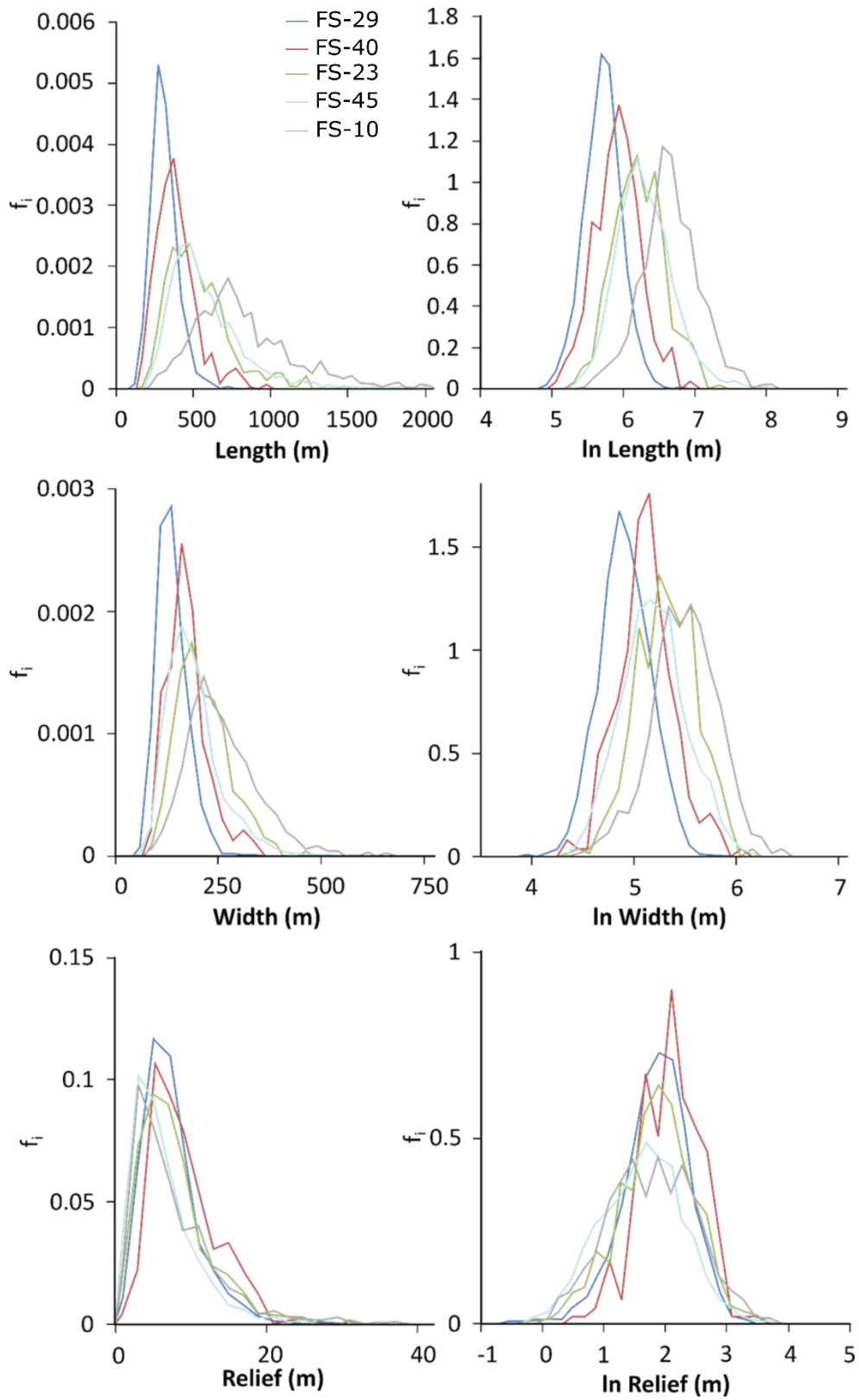
863

864

865

866

Figure 6

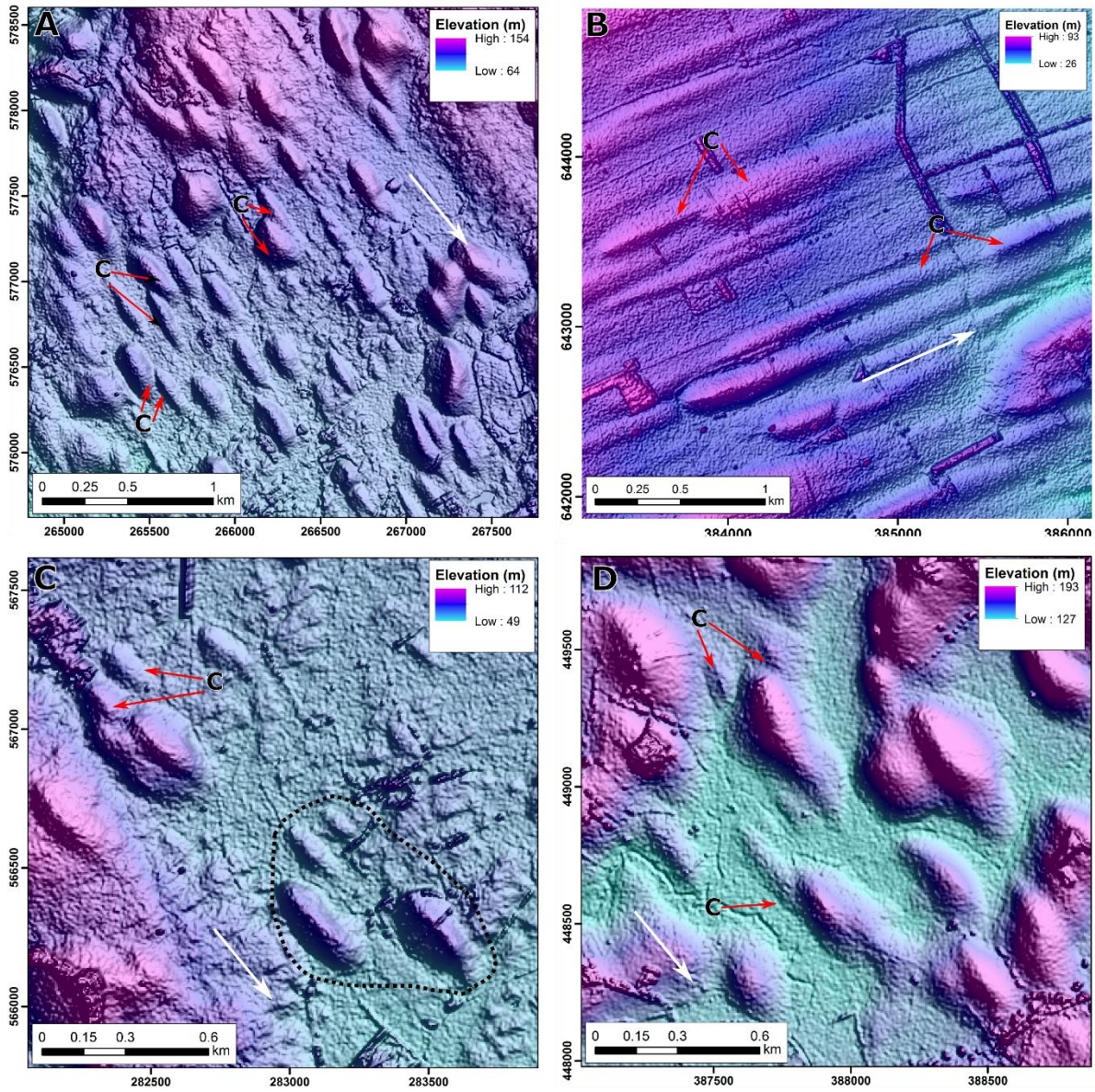


867

868

869

Figure 7



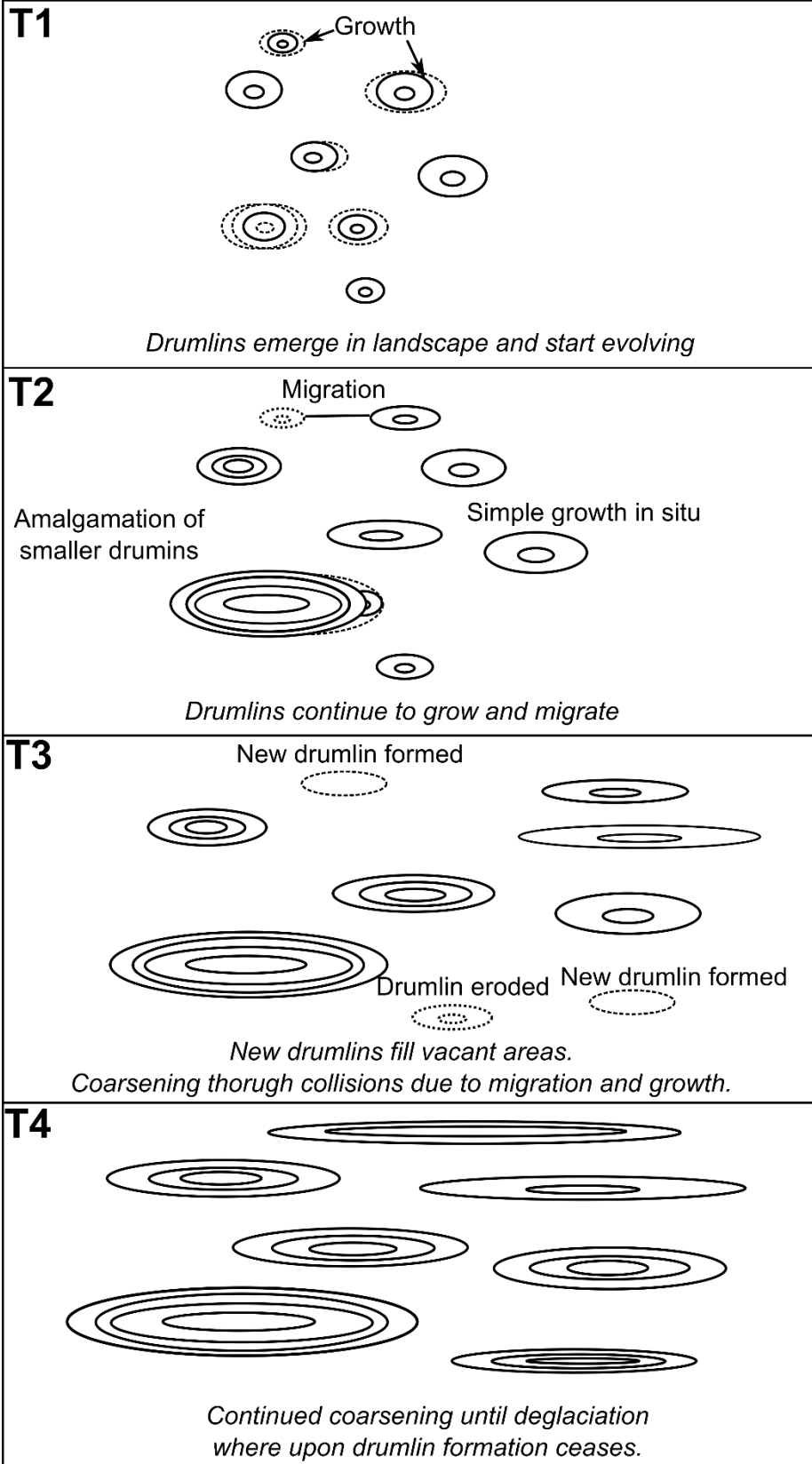
870

871

872

Figure 8

Ice Flow Direction



873

874

Figure 9